



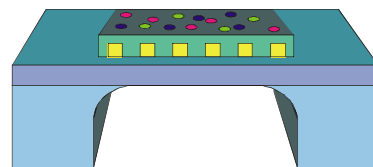
Development of Micro Analytical Vapo^r_{SAND2006-5301P}

Sensor Systems

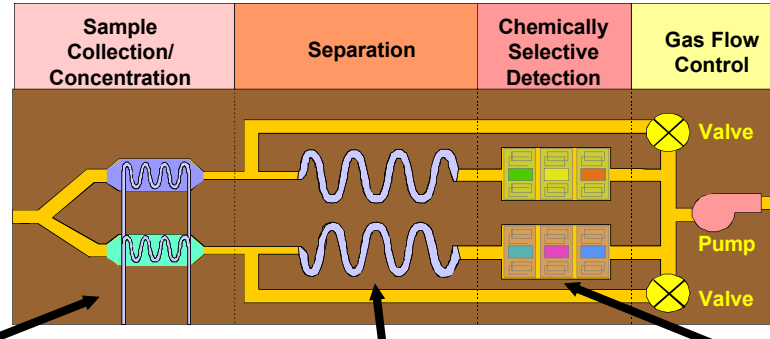
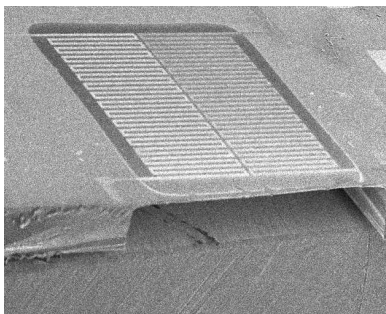
**R.J. Simonson
Sandia National Laboratories
Albuquerque, NM**

**Acknowledgements are due to many members of the
μChemLab team including Doug Adkins, Jim Barnett, Matt
Blain, Joy Byrnes, George Dulleck,, Pat Lewis, Ron
Manginell, Alex Robinson, Jim Spates, Al Staton, Dan
Trudell, Joshua Whiting, and Dave Wheeler**

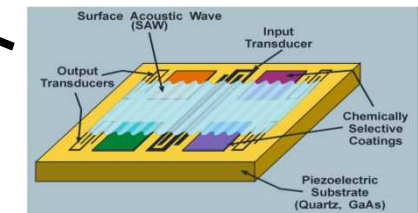
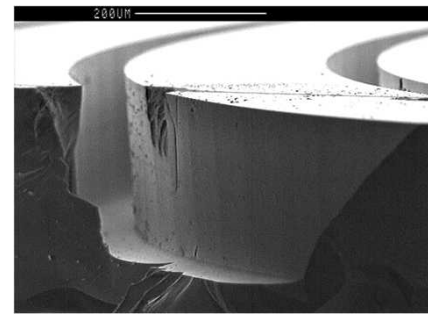
Hand-held chemical analysis system that uses three microfabricated stages.



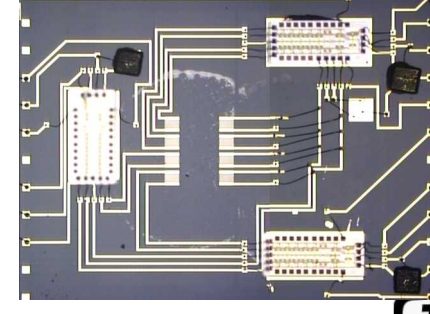
Preconcentrator accumulates species of interest



Gas Chromatograph separates species in time



Acoustic Sensors provide sensitive detection



Sandia
National
Laboratories



Chemical Selectivity at Each Stage is Driven by Phase Partitioning of Analytes

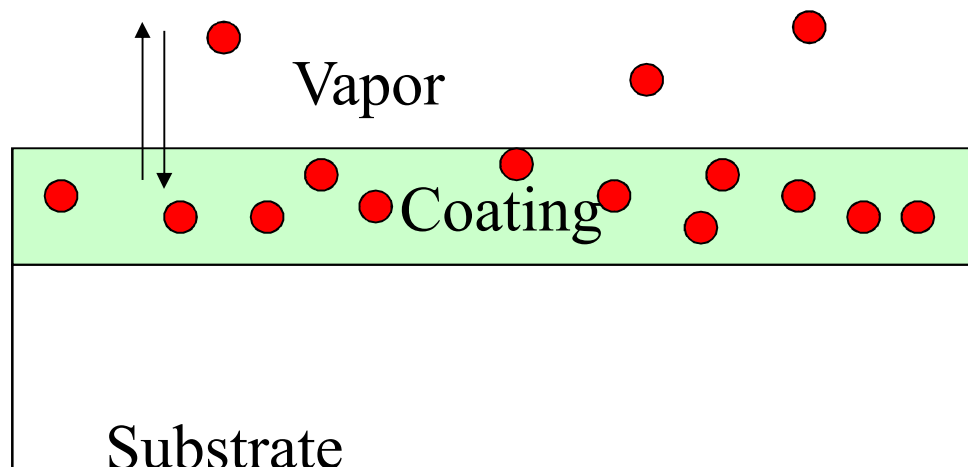
- Partitioning between phases is driven by difference in Gibbs free energy of the molecules in each phase – *but ignore kinetics at your own risk!*

$$K = C_s/C_v = \exp[-\Delta G_s/RT]$$

Where C_s = Concentration in surface coating

C_v = vapor concentration

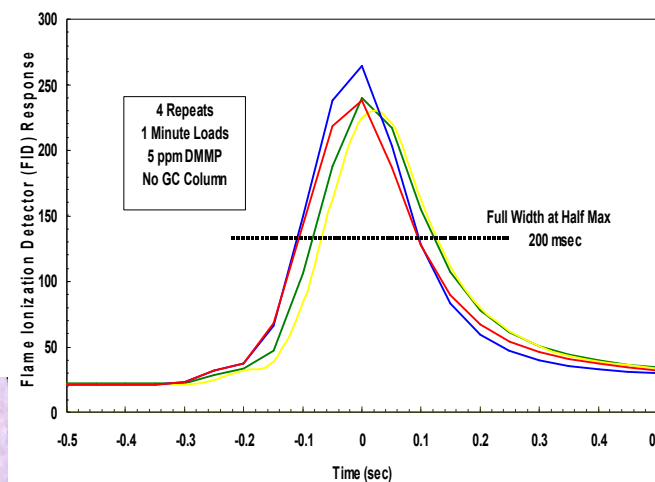
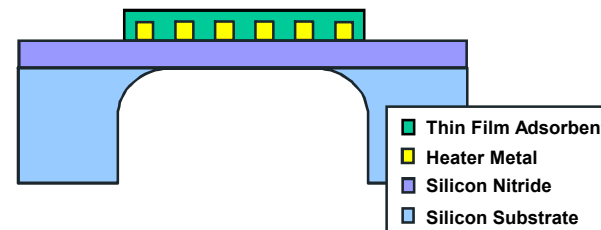
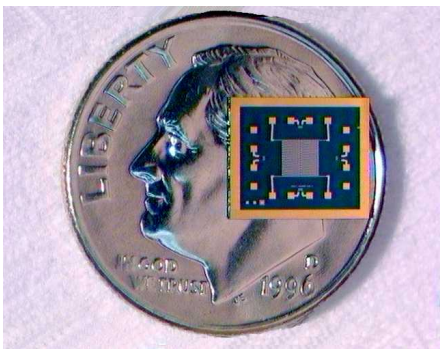
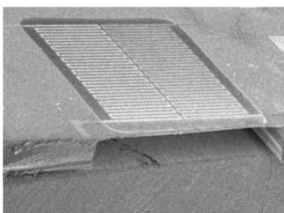
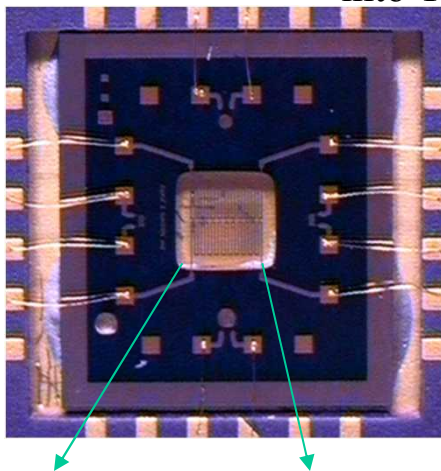
ΔG_s = Gibbs free energy of solvation in coating



Preconcentrator

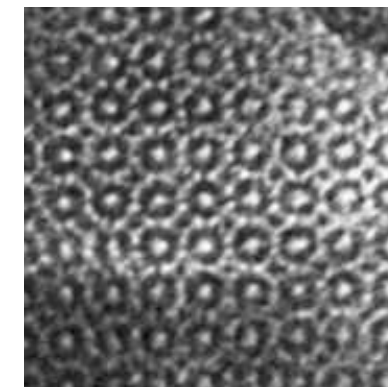


Thermally Isolated Heater Provides Rapid and Low Power Thermal Desorption of Analyte Collected into Thin Film Adsorbent

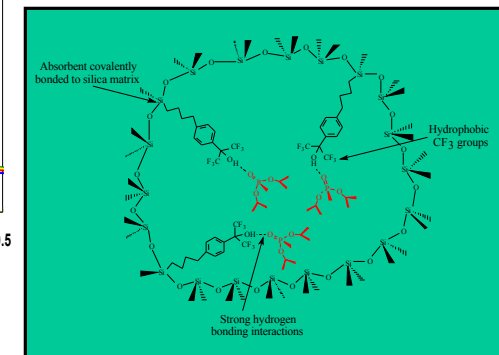


Rapid Thermal Desorption from
Micromachined Preconcentrator

Novel Sol-Gel Techniques Provide Thin Film Adsorbents with High Uptake and Chemical Selectivity



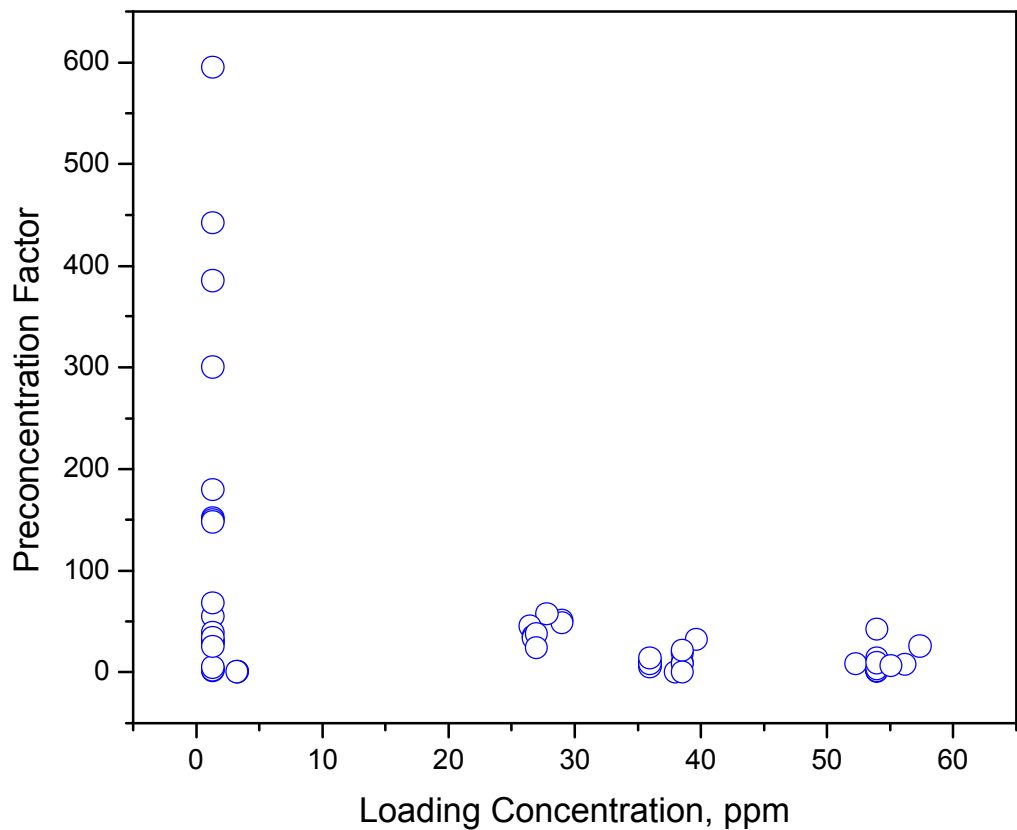
Tailored Porosity



Tailored Surface Chemistry

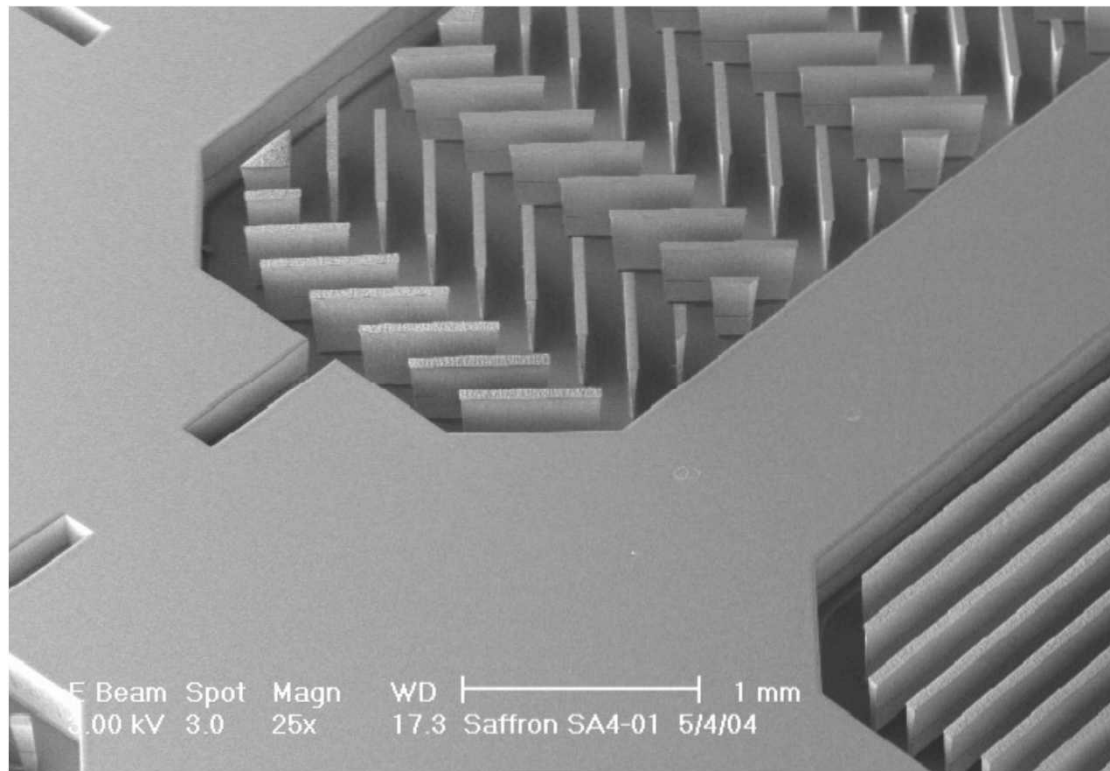
Planar Preconcentrator: Example

- Carboxen/PDMS coating on planar PC
- Target compound exposure, FID detection
- Desired preconcentration: $\sim 1000\times$
- Results:
 - “Best” preconcentration at lower loading concentration
 - Preconcentration effectiveness can vary by orders of magnitude at nearly constant concentration, depending on operating parameters





Improving the micro Preconcentrator

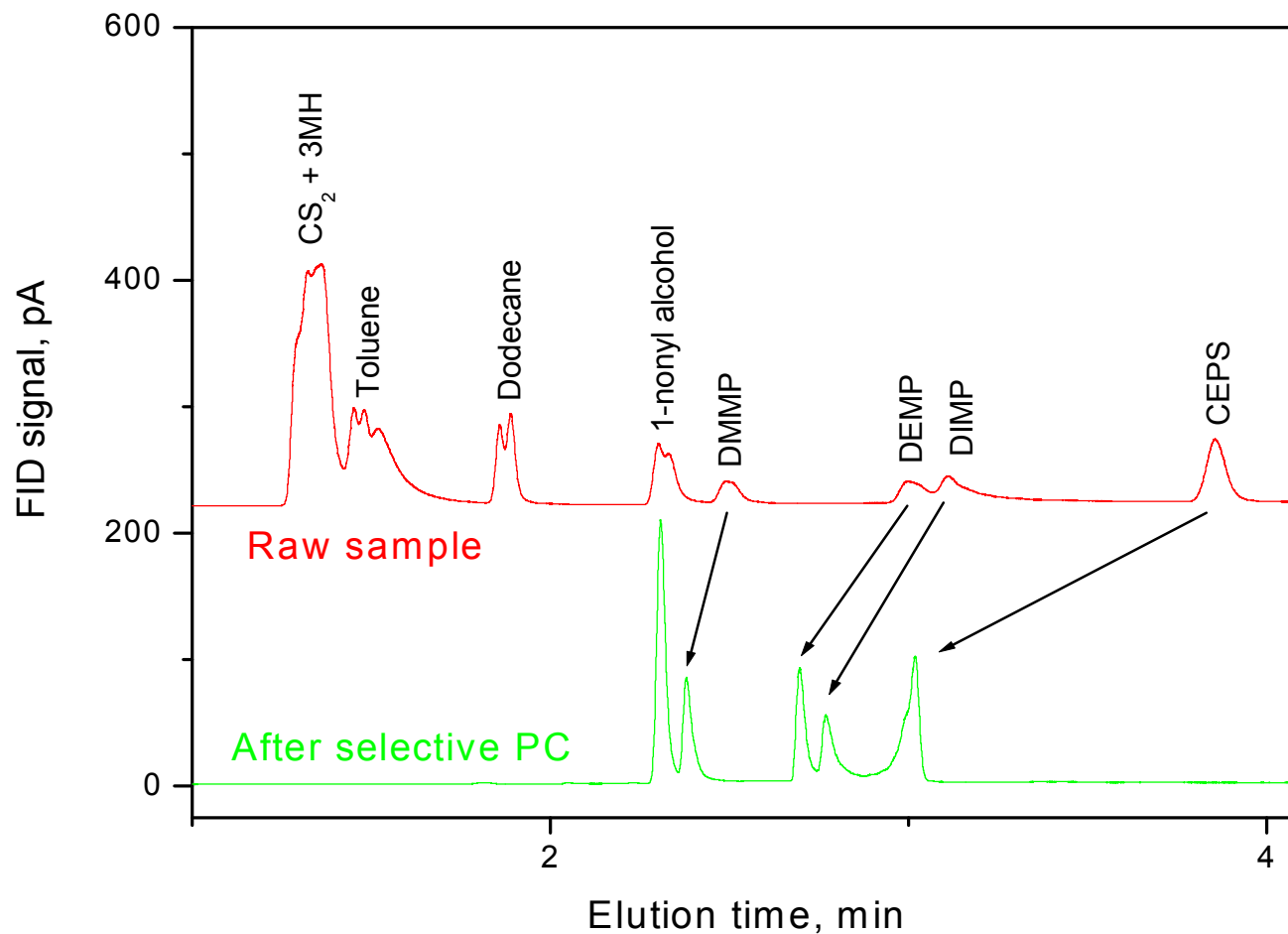


- Microfabricated structures can be designed to increase capture efficiency and adsorption capacity, while matching flow impedance to micro GCs.
- These low thermal mass structures are combined with high surface area coating materials with tailored porosity and chemical functionality.



Preconcentrator Coatings Provide Chemical Selectivity

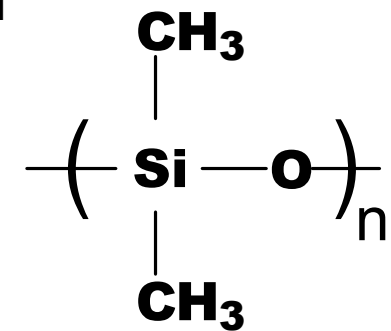
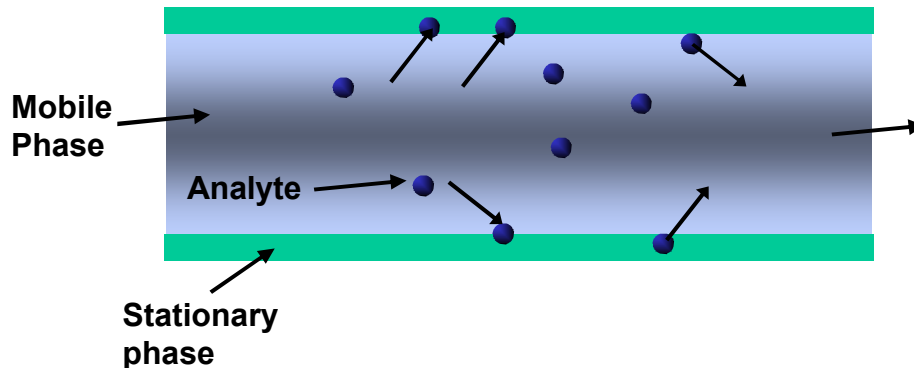
- Selective preconcentration reduces the possibility of oversaturation (overload) of low-volume-ratio GC stationary phases, improving separation and lowering false alarm rates.





Separation Strategies using the GC Column

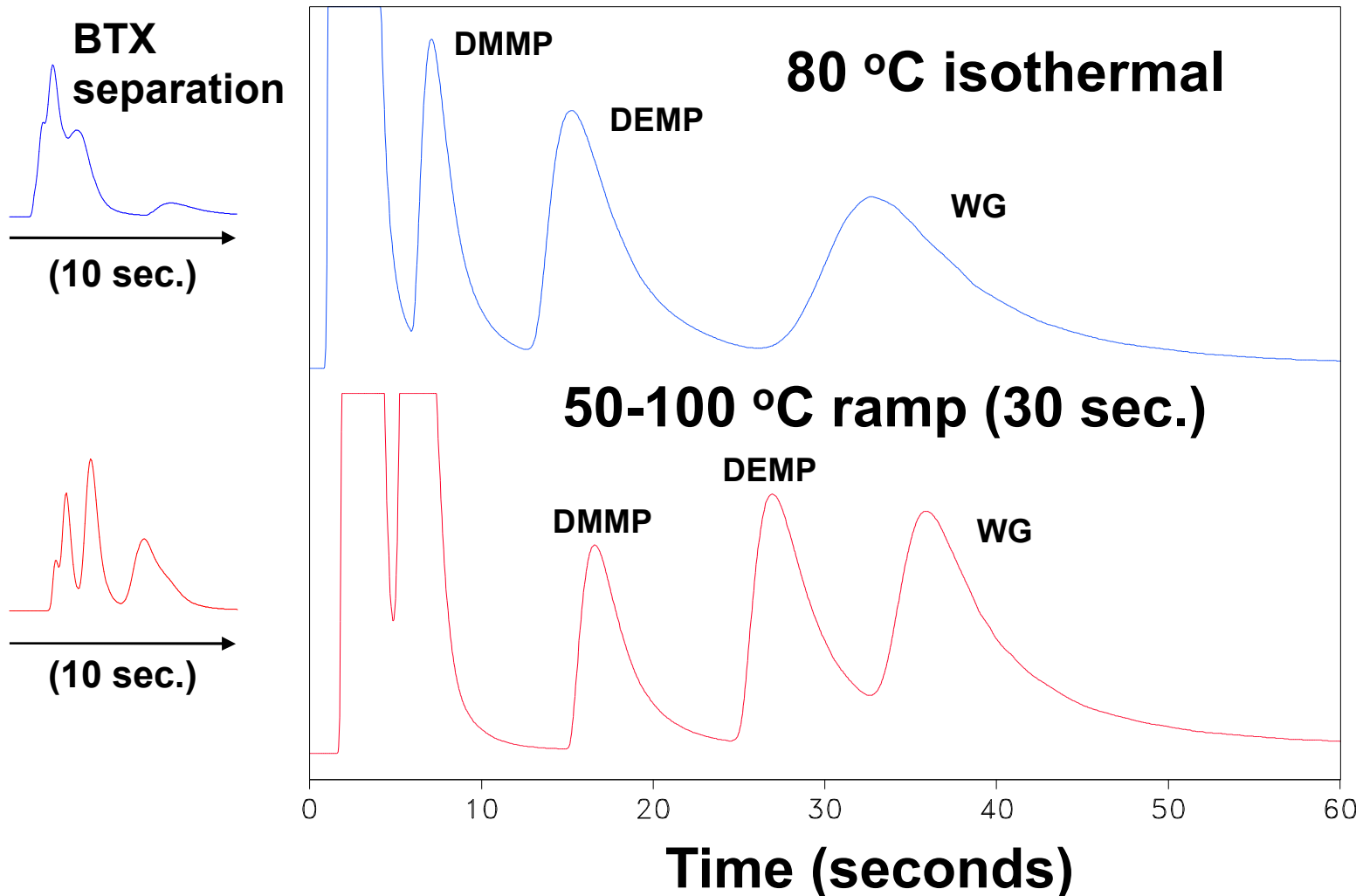
- Separation strategies involve the interaction of the analyte and the column coating or stationary phase
- GC column stationary phase: PDMS coating linked to Si-OH terminations on column surface through TEOS-based sol



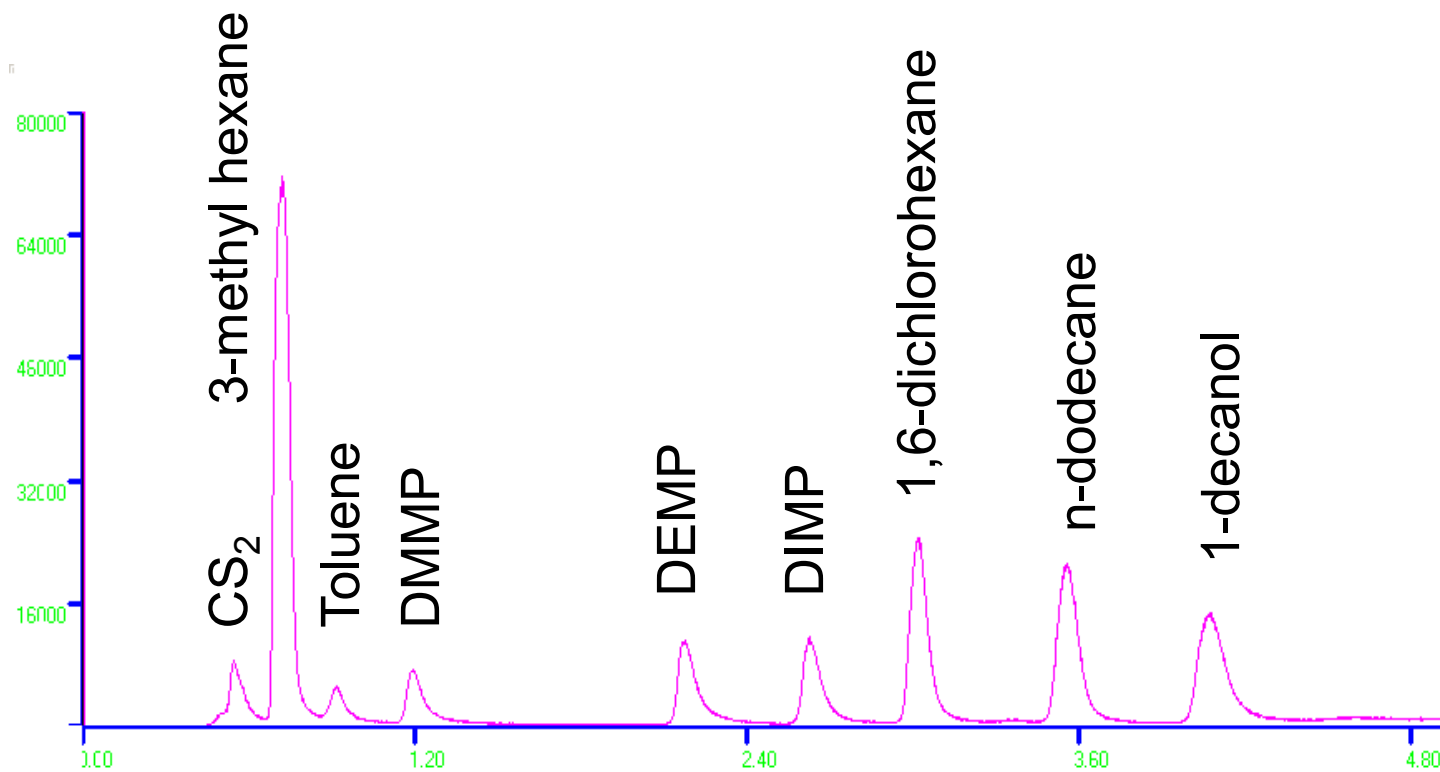
Analytes are repeatedly adsorbed/desorbed as they move through the column

Analytes are separated due to slight differences in their adsorption and desorption rates

Temperature Ramp Chromatography Enhances Separation Efficiency



The Goal: *FAST* Separations of Toxic Agents



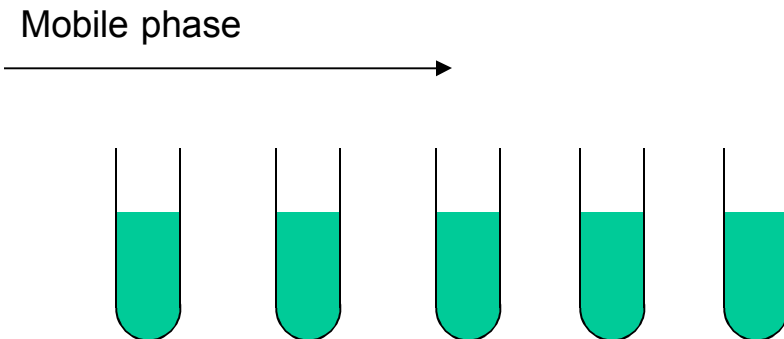
- Mixture of 4 CWA surrogates and 4 interferent compounds separated in less than **4 seconds**.
- High speed separation uses fast carrier at high u as well as temperature programming



Capillary GC Separations: Some concepts

- WHO CARES?
- Firefighters, police, emergency responders for industrial accidents or terrorist attacks involving chemical release.
- Soldiers on the ground who may be subject to chemical attack.
- GC separation of compounds vastly improves accuracy of chemical identification. Important if you have to wear gas masks and protective clothing.
- If you have to put on a gas mask, you need to know quickly.
- Separation *EFFICIENCY* and *SPEED*

Capillary GC Separations: Some concepts

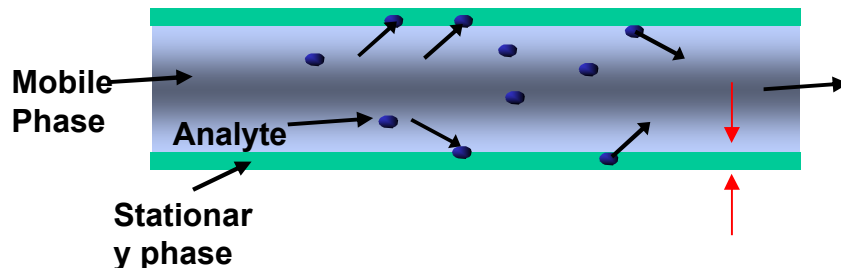


Theoretical plates:
Model column as series of reservoirs, assuming liquid-vapor equilibrium at each step

Height equivalent to a theoretical plate, H : Length increment of a continuous column that is required to establish equilibrium between vapor and the liquid wall coating.

$$H = f(r, d_f, T, \text{partition coefficient } K, \text{gas velocity } u)$$

Goal: Minimize H vs. column length and *time*



d_f = film thickness
 r = column diameter
 L = length



Capillary GC Separations: Concept and terms

Gas flow velocity through the column: u (m/sec)

Retention time, t_R : Time required for a compound to transit the column (sec)

Unretained peak transit time: $t_M = (\text{column length})/u$

Retention factor (dimensionless): $k = (t_R - t_M)/t_M$

The retention factor is a ratio of time spent in the stationary phase vs. time spent in the gas phase. Depends on partition coefficient, K , and phase thickness df . Also called a “capacity factor”.

For open tubular (round) columns, **H vs. u** (at constant T , r , df , and K) is described by the **Golay equation** (1958):

$$H = B/u + Cu$$

Where B and C are constants.

Note that at low values of u , $1/u$ is large, the B term dominates, and H increases.

At large values of u , the C term dominates and H again increases.

At some intermediate value of u , there will be a minimum in H (desired).



The Golay Equation: Some eye-glazing detail

$$H = B/u + Cu$$

- B term describes peak broadening due to diffusion of the solute vapor in the carrier gas:

$$B = 2 D_g$$

Where D_g = binary gas diffusion coefficient (cm²/sec)

- C term describes resistance to mass transport due to retention in the gas phase (viscous drag) + resistance in the stationary phase (retention in soln.):

$$C = C_g + C_{liq}$$

$$C_g = r^2(1 + 6k + 11k^2)/\{24D_g(1 + k)^2\}$$

$$C_{liq} = 2kd_f u/\{3(1 + k)^2 D_{liq}\}$$

In the limit of small d_f (thin films), C_{liq} becomes negligible.



The Golay Equation: Freshman Calculus

$$H = B/u + Cu$$

- To find the maximum separation efficiency (minimum H), differentiate H with respect to u and set equal to zero, assuming d_f is small:

$$dH/du = -B/u^2 + C_g = 0$$

So

$$U_{\text{optimal}} = (B/C_g)^{1/2}$$

$$= (4D_g/r)(1 + k)[3/(1 + 6k + 11k^2)]^{1/2}$$

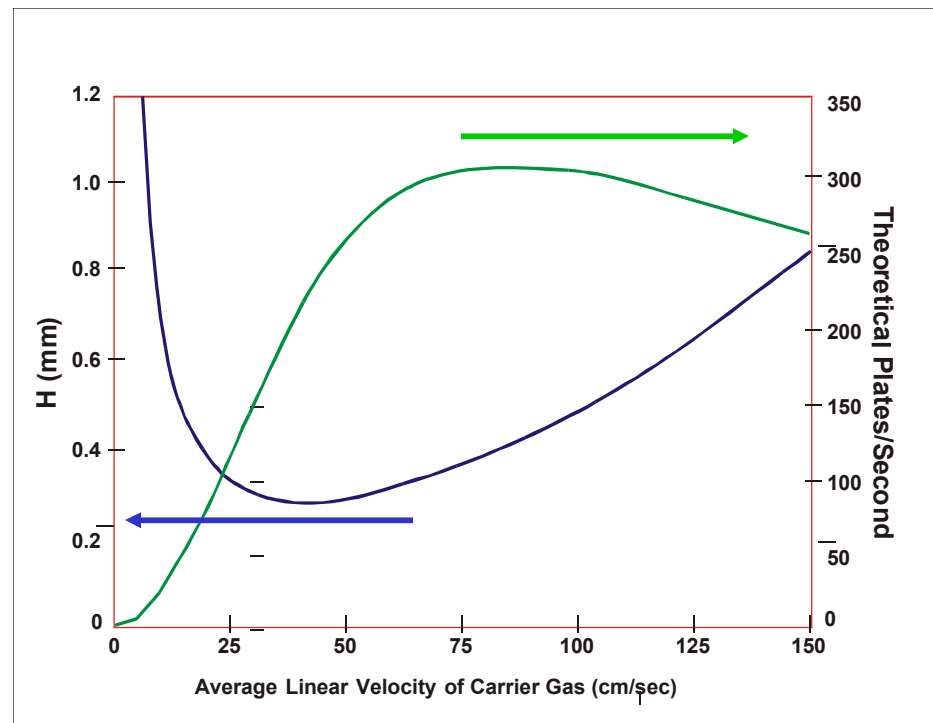
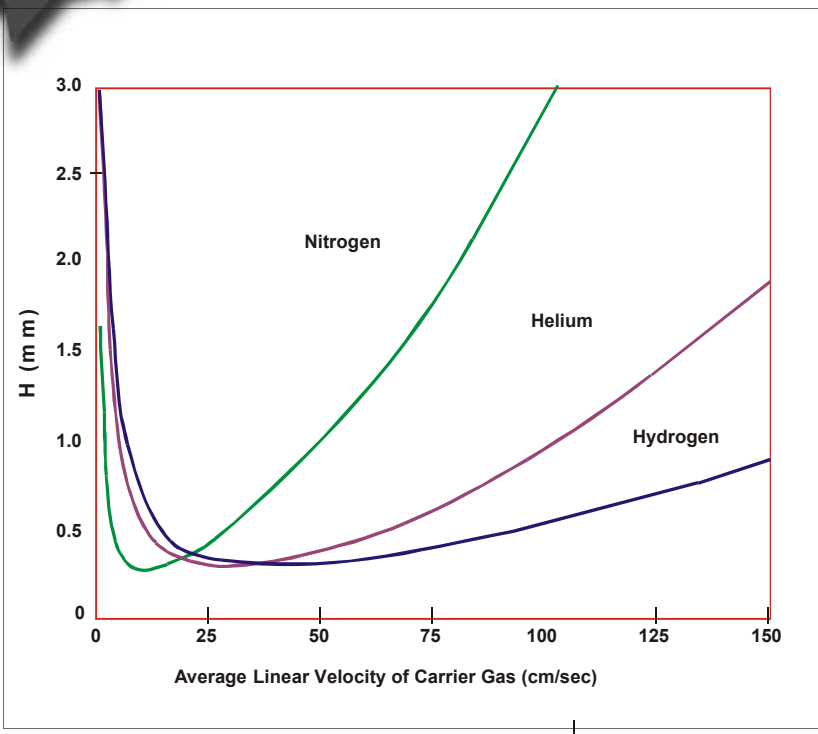
So what? Smaller r requires faster u, but high flow is harder to achieve at small r due to gas viscosity.

- To find the maximum efficiency of the column, substitute optimal value of u back into the expression for H(u) and do some messy algebra:

$$H_{\text{min}} = r \{(1 + 6k + 11k^2)/3(1 + k)^2\}^{1/2}$$

Small diameter columns (small r) minimize H *if you can force the gas though fast enough.*

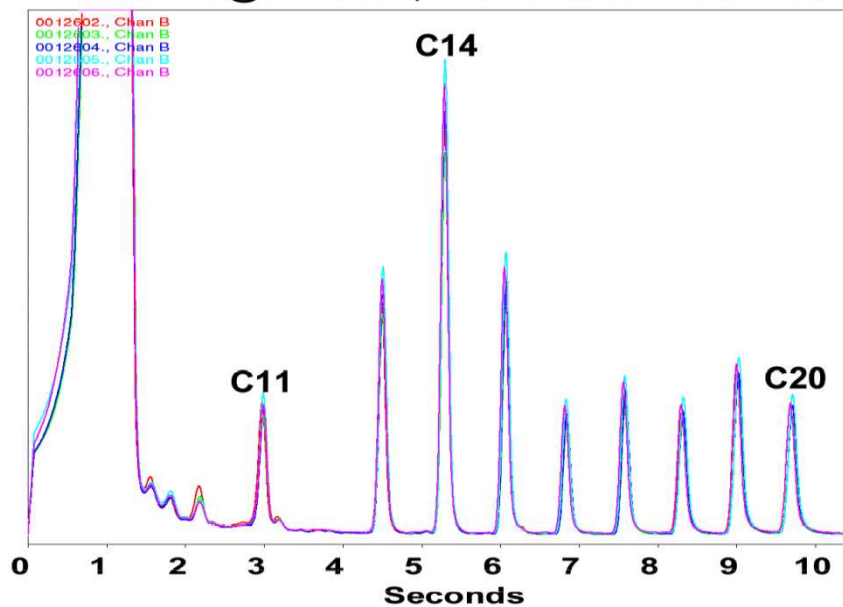
Carrier Gas effects on GC efficiency



- Lowest viscosity carrier (hydrogen) allows for widest flow rate (pressure) operating range, allowing best compromise in both H and plates/sec
- Shorter column and high flow rate = best separation at high speed

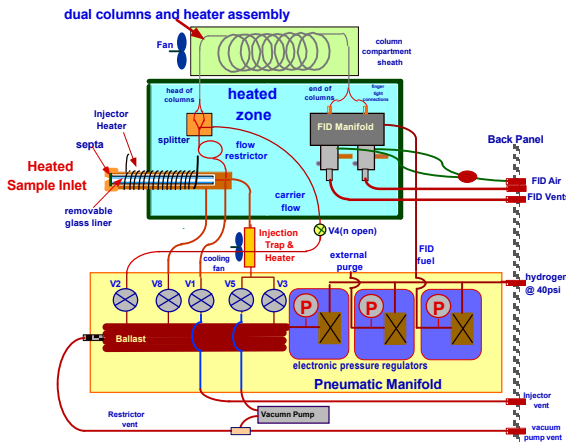
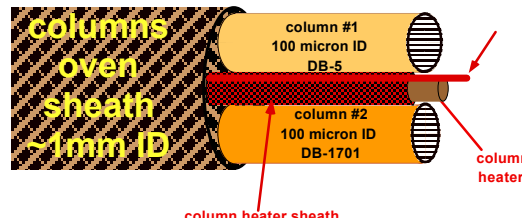
LSU/ASI's current microFAST GC/ system: Rapid separations using fast temperature programming Speed and Broad Compound Range

5 Replicate microFAST GC Analyses of Semivolatile Std.
90°C to 270°C @ 20°C/sec, one meter DB1701 Column



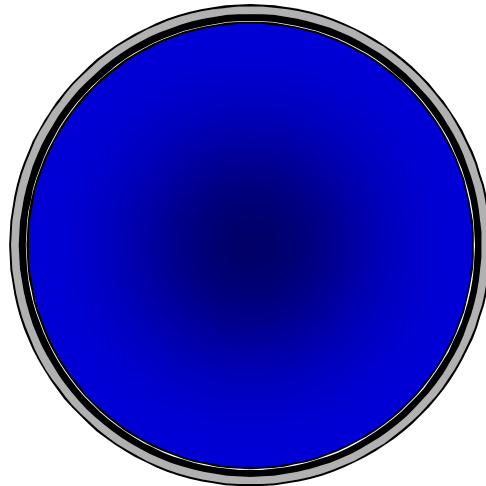
microFAST GC analytical columns assembly

Column Types:
 -100 to 320 micron ID
 -1 to 3 meters in length
 -either open tubular or PLOT

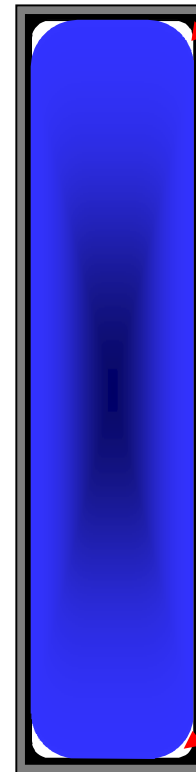




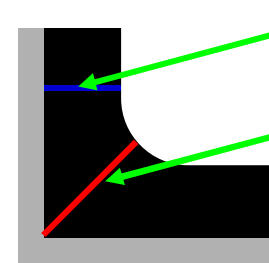
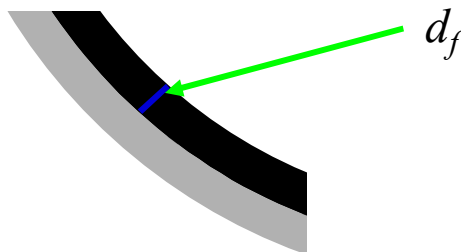
Round vs. HARM columns



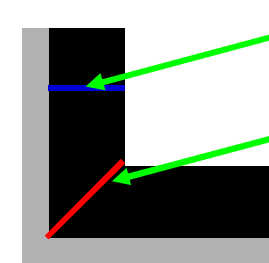
- Flow restriction and performance limited by radius
- Film deposition is uniform



- Flow restriction controlled by height
- Performance limited by width
- End effects
 - Film deposition often results in thicker phases in the corner
 - Dead spaces in corners



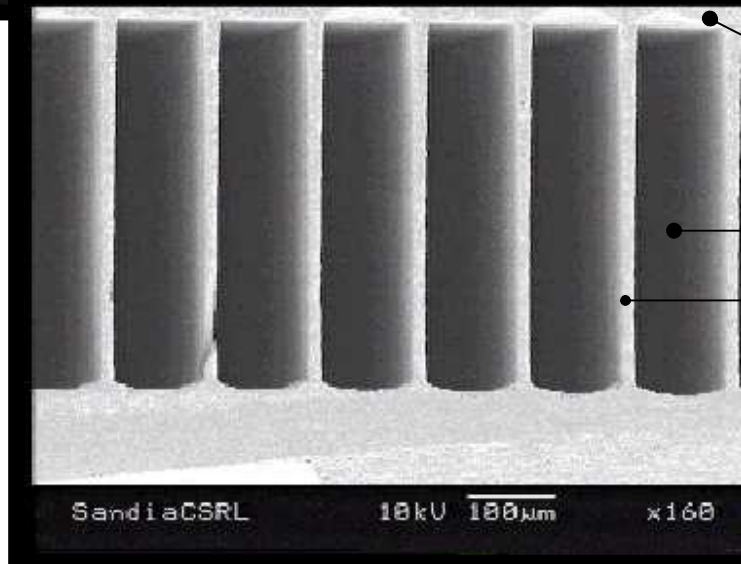
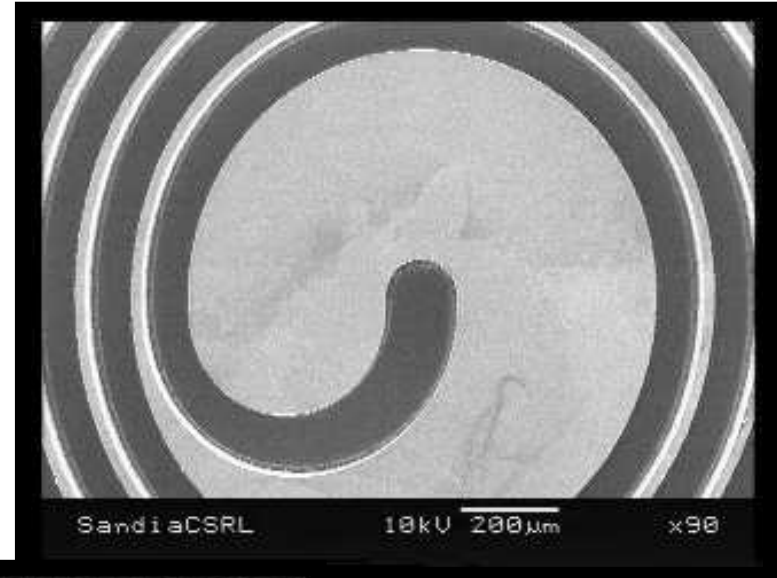
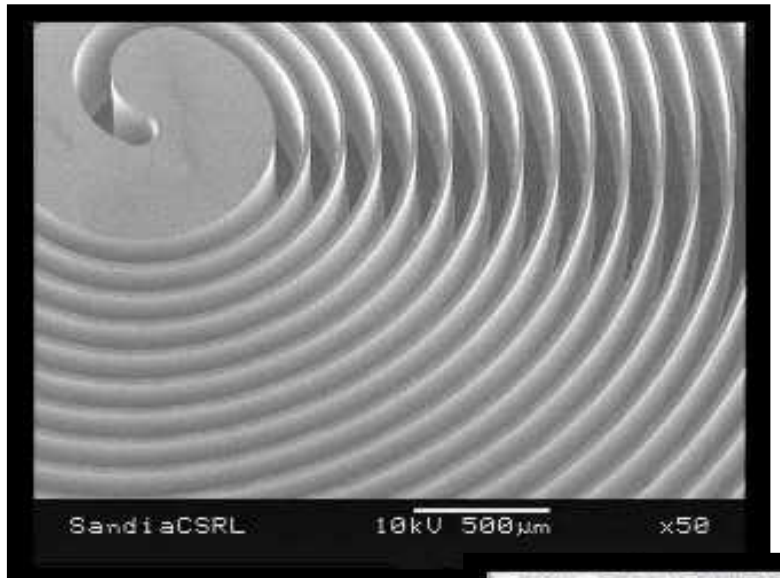
$$d_f, \sqrt{2}d_f + (\sqrt{2} - 1)r$$



$$d_f, \sqrt{2}d_f$$



Deep Reactive Ion Etching Capability used to Fabricate Gas Chromatograph Columns



- 25 μm walls
- 100 X 400 μm profile
- 1 m length
- 1 cm^2 footprint



Golay equation for Rectangular GC columns

1st 3 terms model column performance, 4th term connects column to system

$$H = \underbrace{\frac{2D_g f_1 f_2}{\bar{u}}}_{\text{Longitudinal diffusion}} + \underbrace{\frac{(1 + 9k + 25.5k^2)}{105(k+1)^2} \frac{w^2}{D_g} \frac{f_1}{f_2} \bar{u}}_{\text{Mass Transport in the Mobile Phase}} + \underbrace{\frac{2}{3} \frac{k}{(k+1)^2} \frac{(w+h)^2 d_f^2}{D_s h^2} \bar{u}}_{\text{Mass Transport in the Stationary Phase}} + \underbrace{\frac{\Delta t^2 u^2}{L(k+1)^2}}_{\text{Extra-Column Band Broadening}}$$

\bar{u} – average linear carrier gas velocity

D_g – binary diffusion coefficient in gas phase

f_1 – Giddings-Golay gas compression correction factor

f_2 – Martin-James gas compression correction factor

k – retention factor

w – channel width

h – channel height

d_f – stationary phase film thickness

D_s – binary diffusion coefficient in stationary phase

L – column length

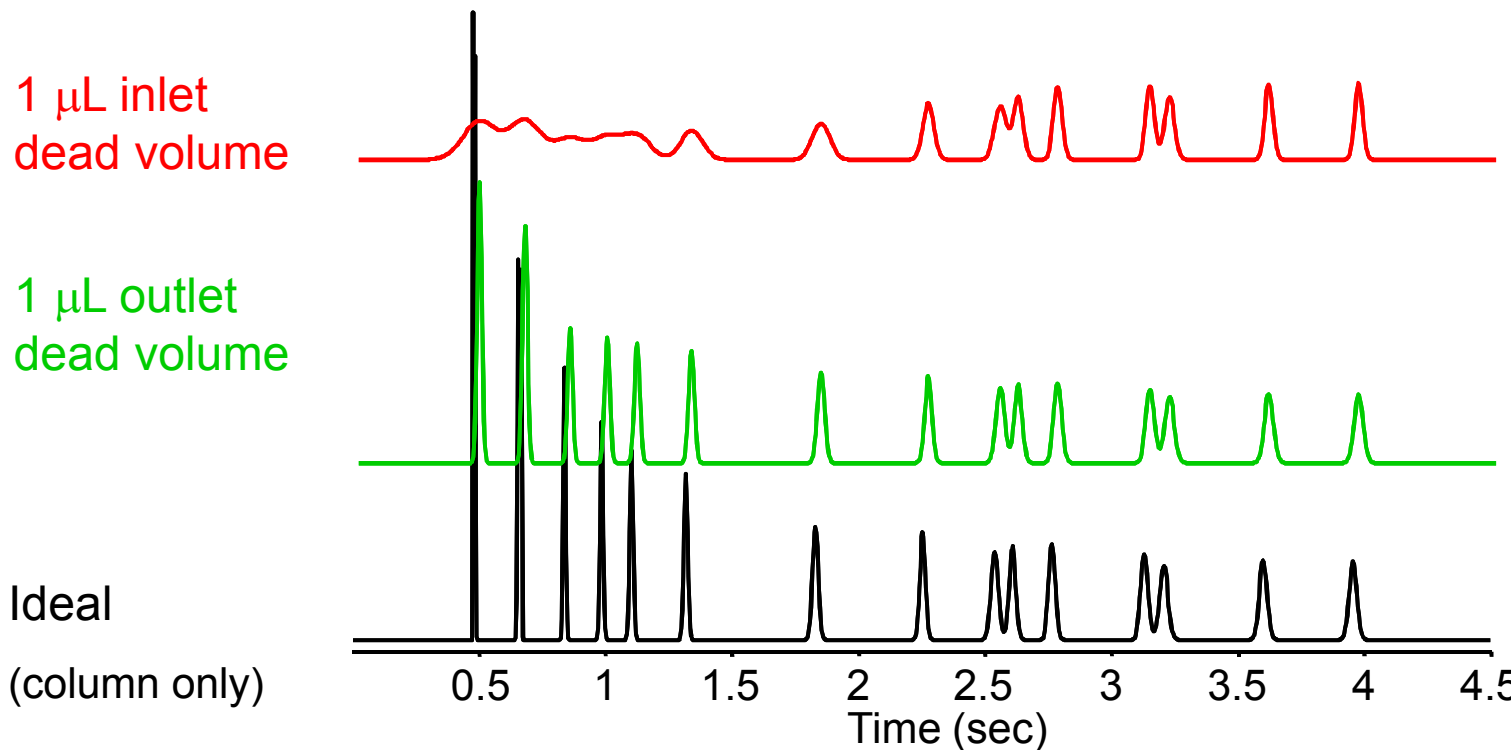
Δt – time correlating to extra column band broadening

$$\Delta t = \frac{\text{inlet (or outlet) volume, cm}^3}{\text{gas flow rate, cm}^3/\text{sec}}$$

Integration Driver: Modeled GC Band Broadening

Ahn and Brandani Model – Dec. 2005

T-programmed 8/8 separation



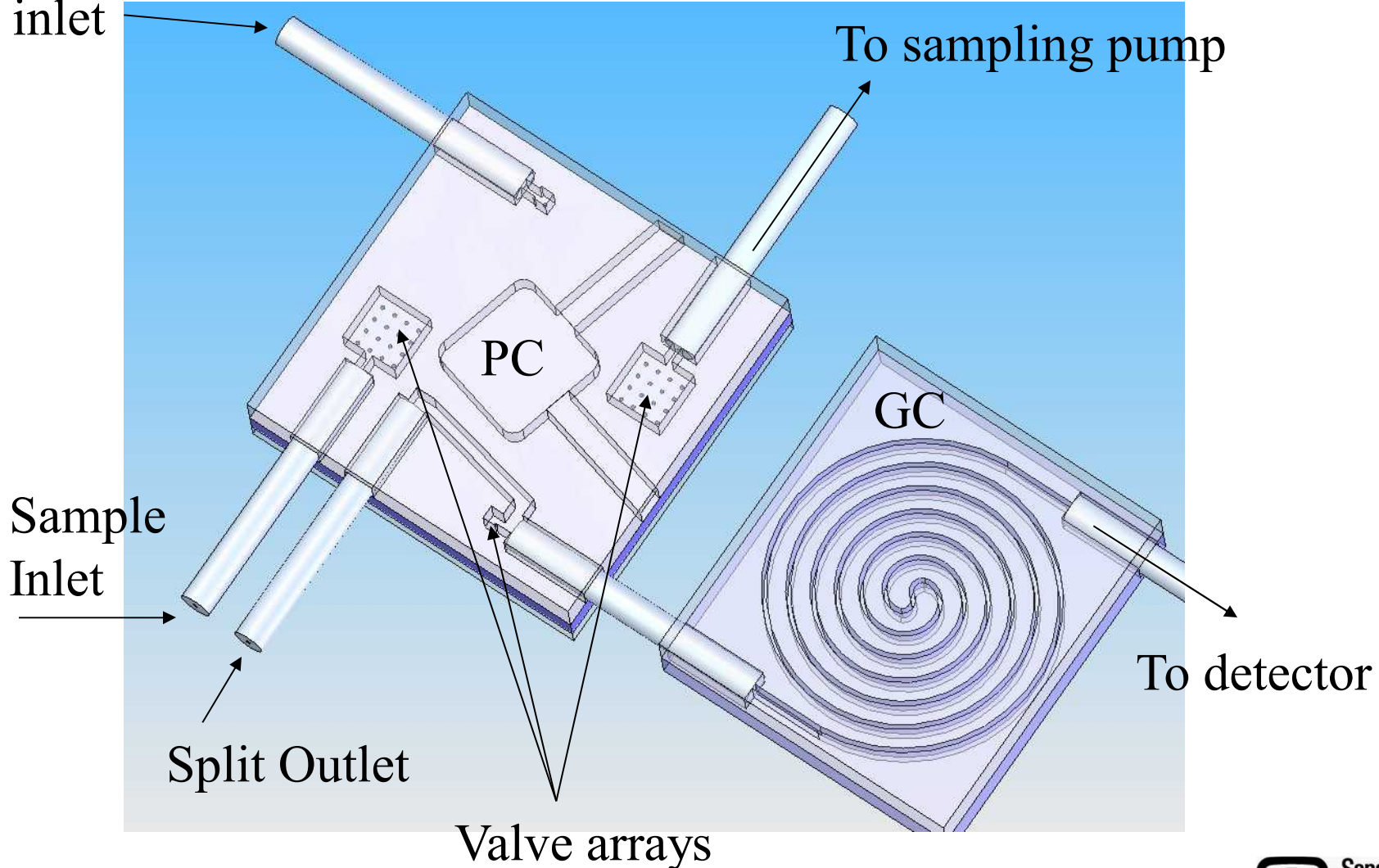
Inlet dead volume costs more than outlet dead volume due to carrier gas compressibility: $(\text{cm}^3/\text{sec})_{\text{outlet}} > (\text{cm}^3/\text{sec})_{\text{inlet}}$



Phase 2 Hybrid Chips

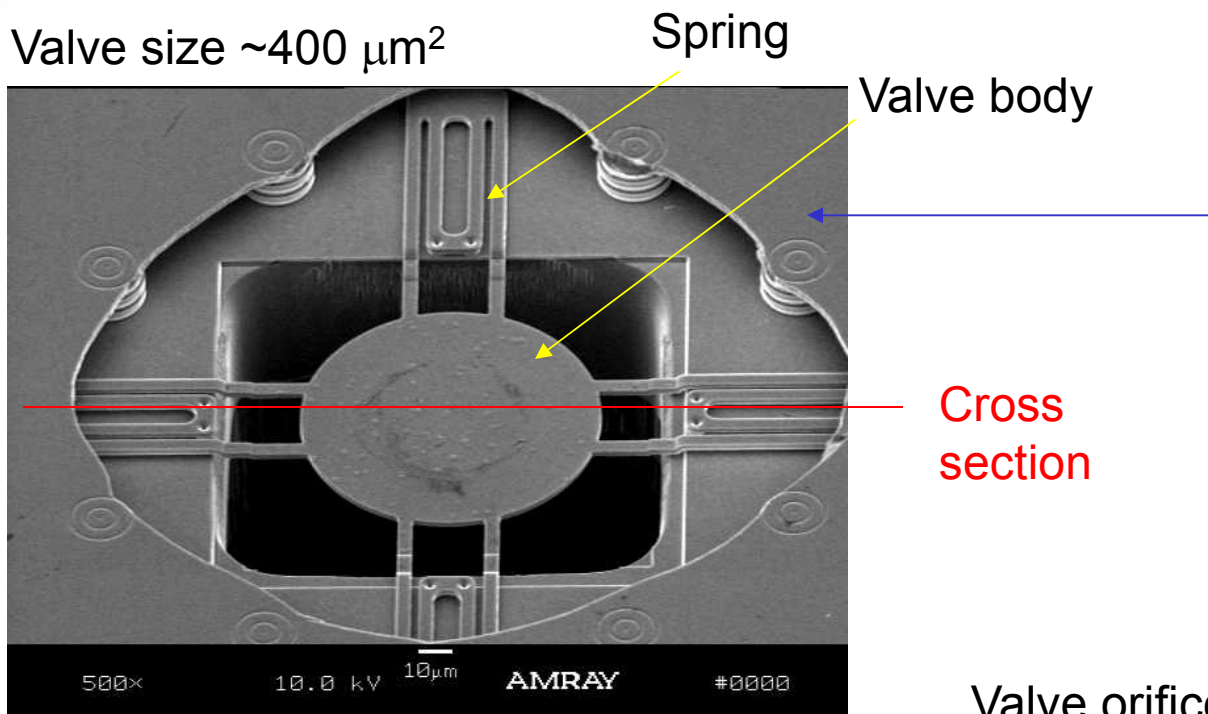
MEMS valves on PC chip limit inlet volume

H_2 inlet



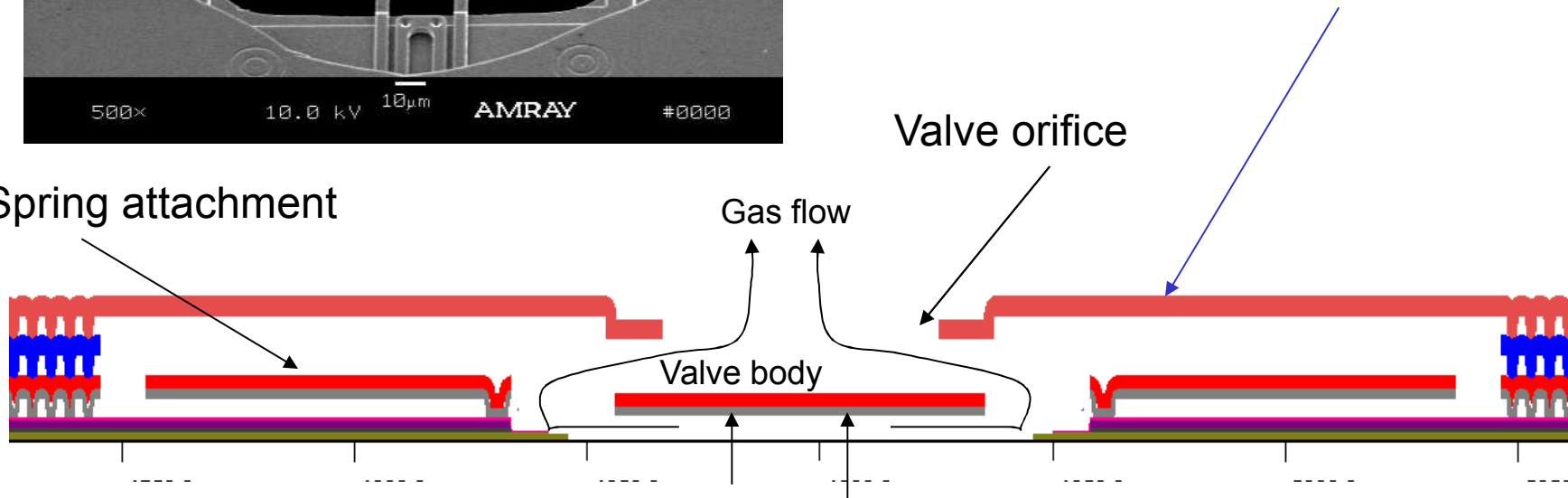
Valve 2 - SUMMiT™ design and fabrication

Valve size $\sim 400 \mu\text{m}^2$

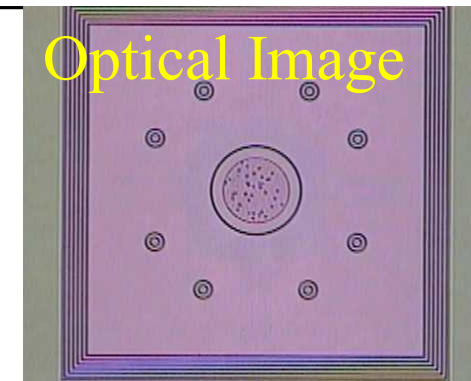
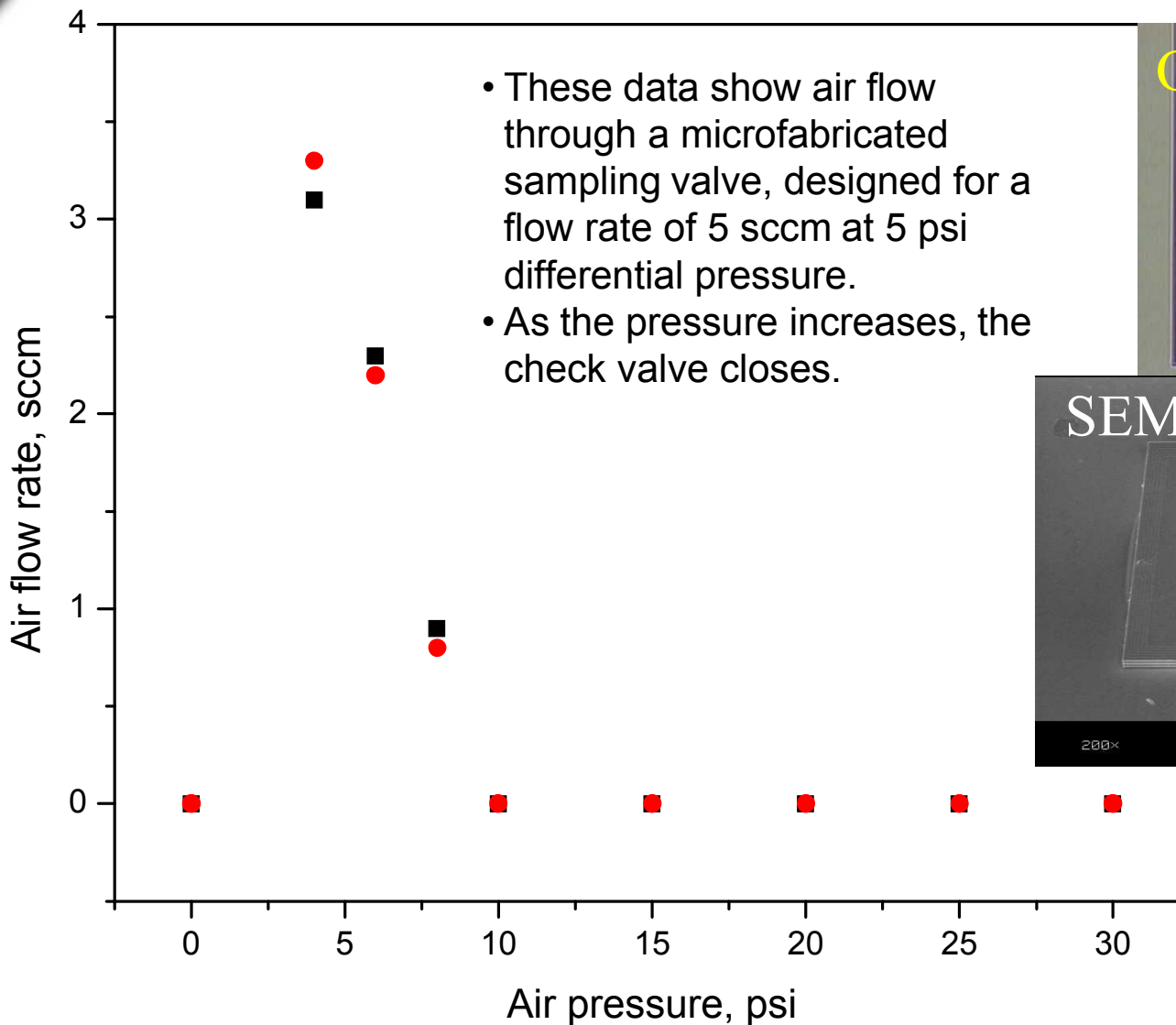


Upper poly-Si layer, which defines the valve orifice, is cut away in the micrograph

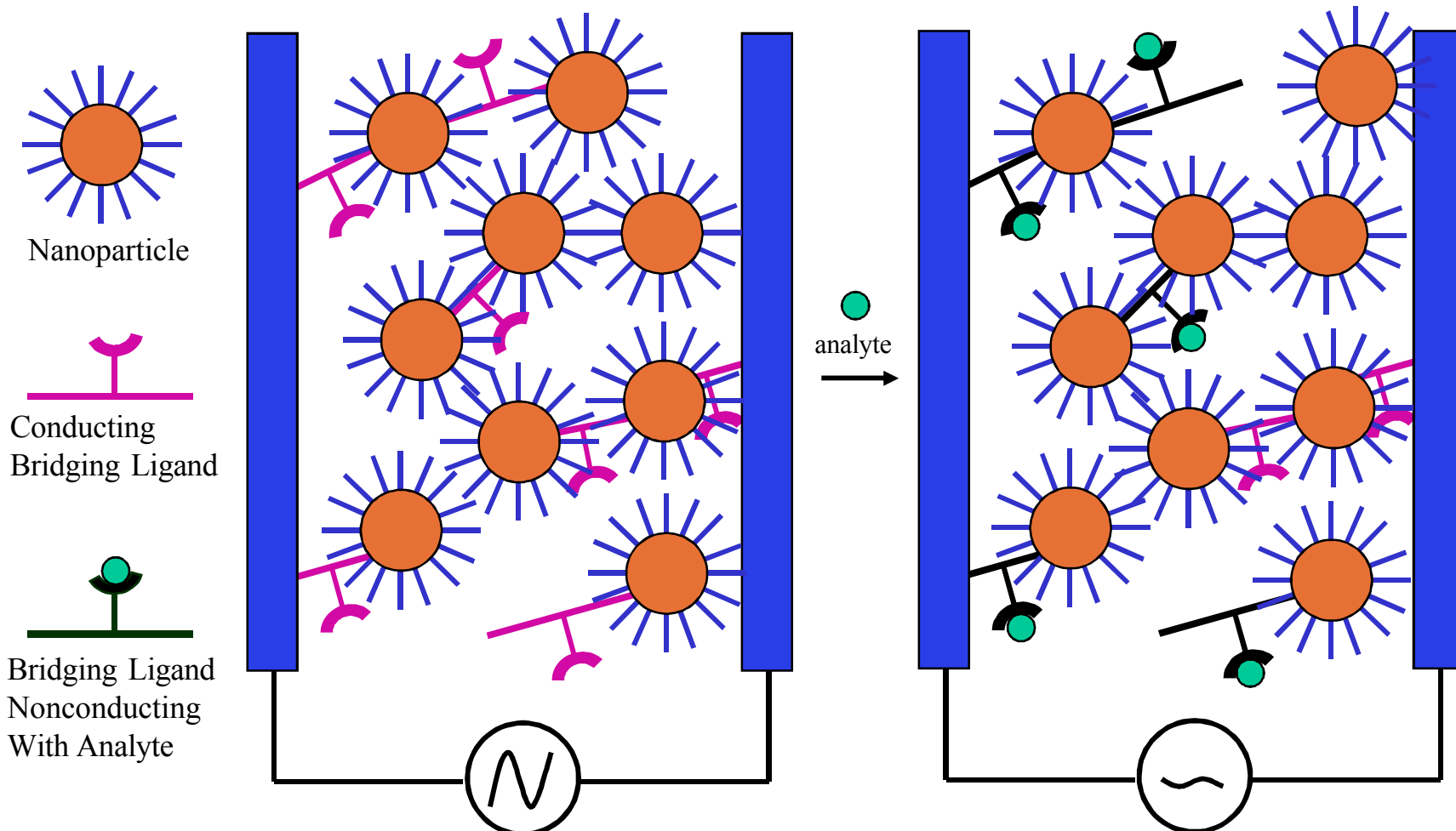
Spring attachment



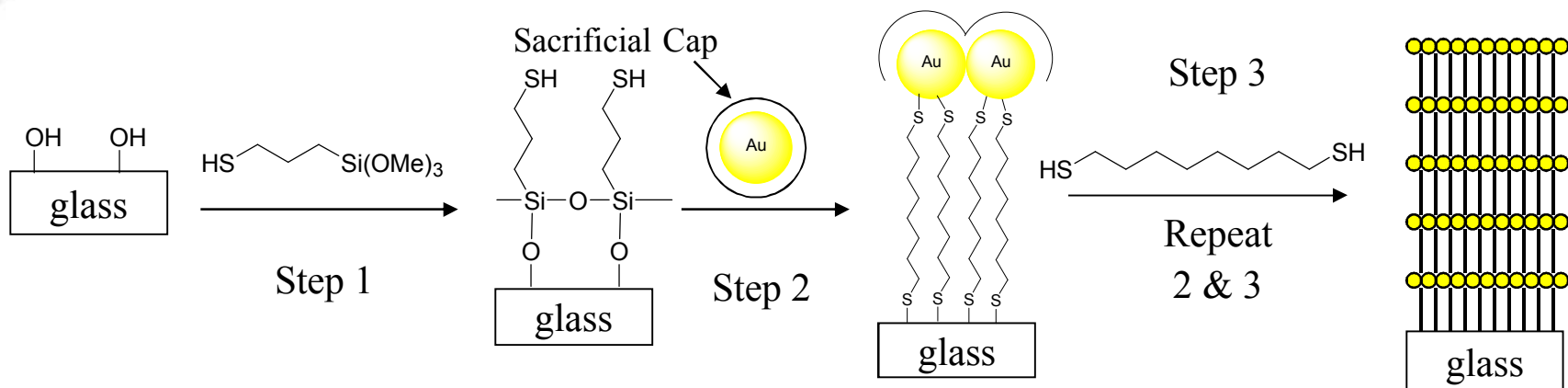
Example Data: Offset Check Valves



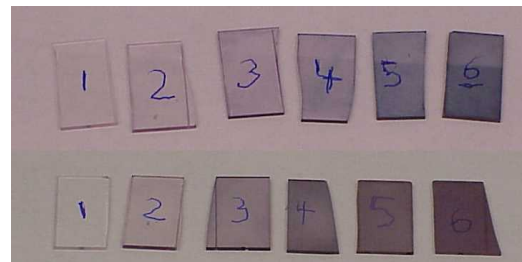
New Detectors for Micro GCs: Nanoparticle/organic composites as chemiresistors



Layer by Layer Resistance Measurements on Glass

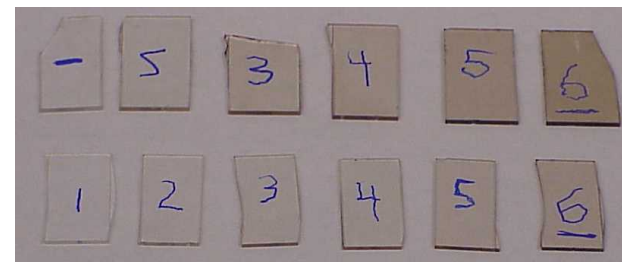


Au/DIH



Au/PE

At/PE



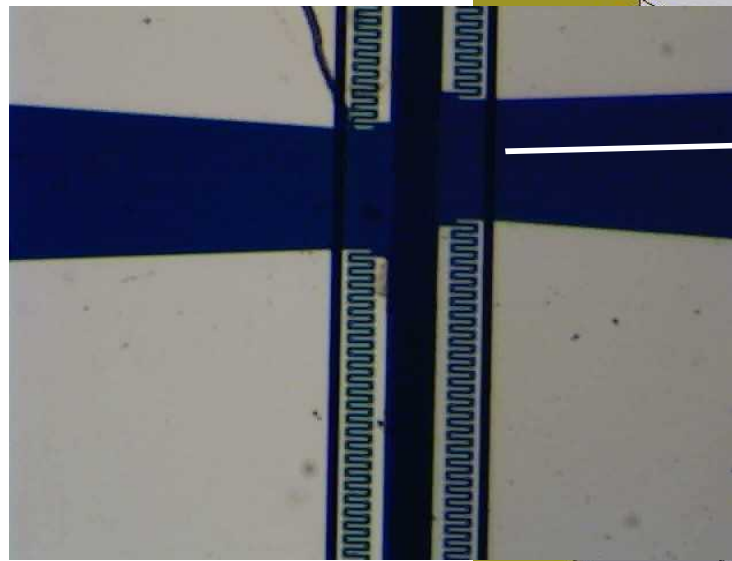
Pt/DIH

- Four point probe measurements of resistance were made, showing decreasing resistance as layers build up

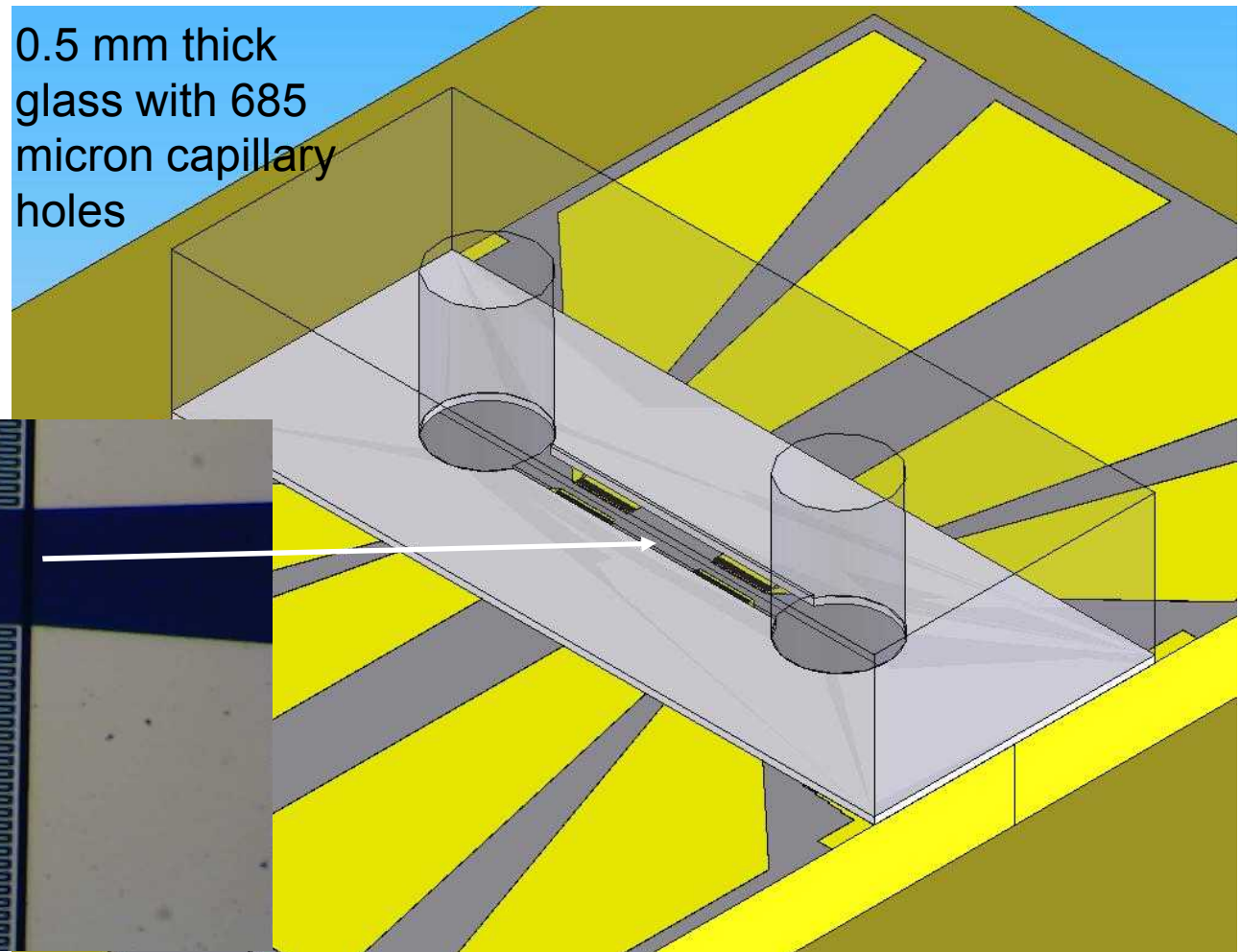


Nanoparticle IDT Arrays

Two quartz nanoparticle IDT chips covered by a flow lid



0.5 mm thick glass with 685 micron capillary holes

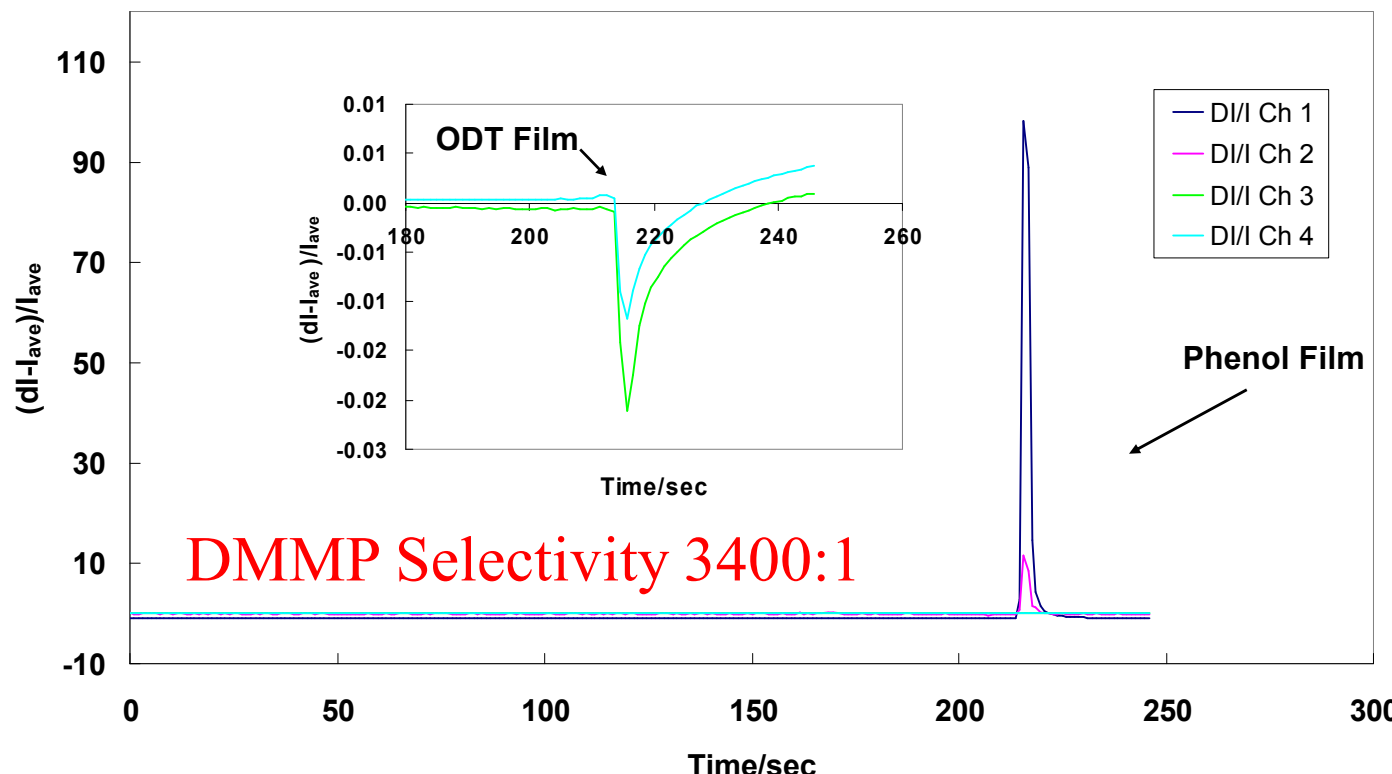


Initial Vapor sensing of DMMP using a protected phenol

Our initial observations during exposure to DMMP show:

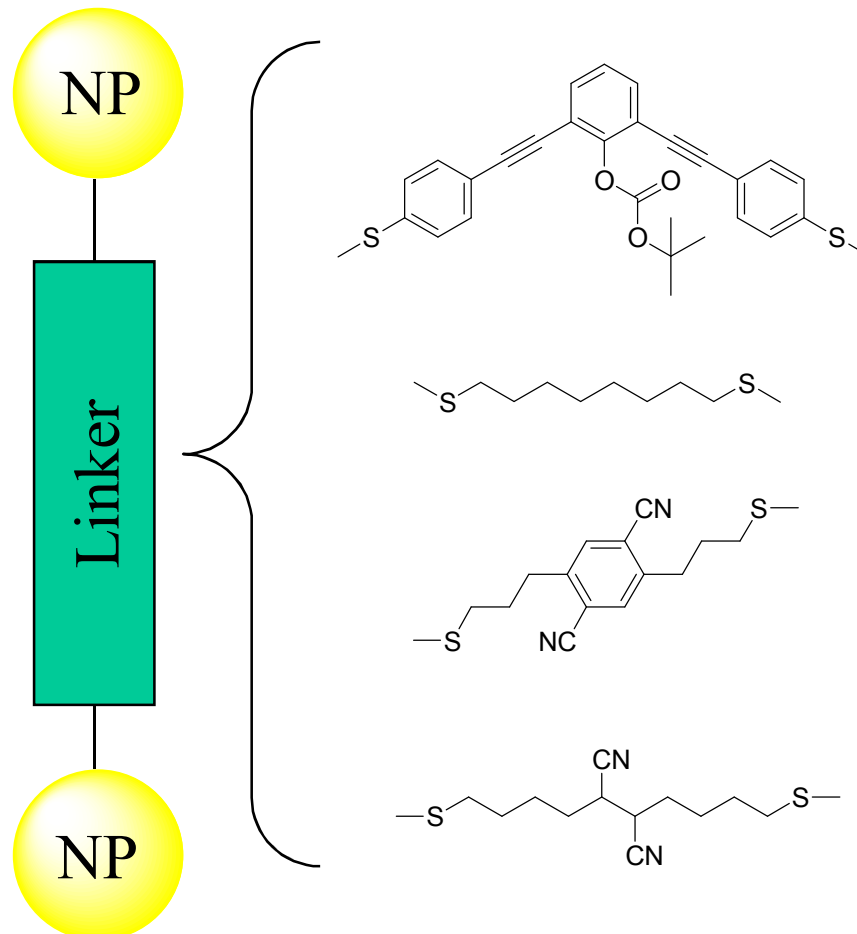
- Protected phenol-Au films have dramatically increased conduction (molecular electronic effect)
- Control ODT-Au films have a slight decrease in conduction (swelling)
- 10⁻⁴ J per detector channel per analysis!**

DMMP vapor from Tenax PC using Boc Protected Phenol Molecule as Ch 1 and Ch 2 and ODT as Ch 3 and Ch 4 both with Au nanoparticles





Additional Sensor Channel Candidates



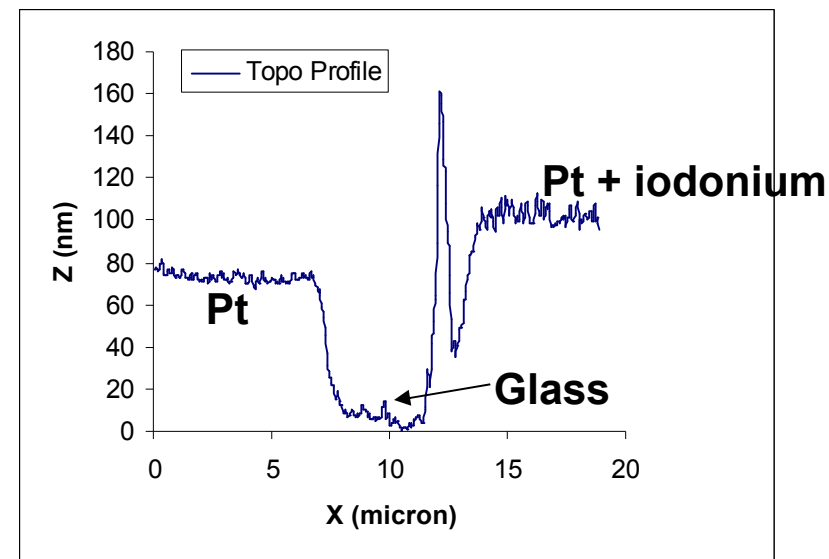
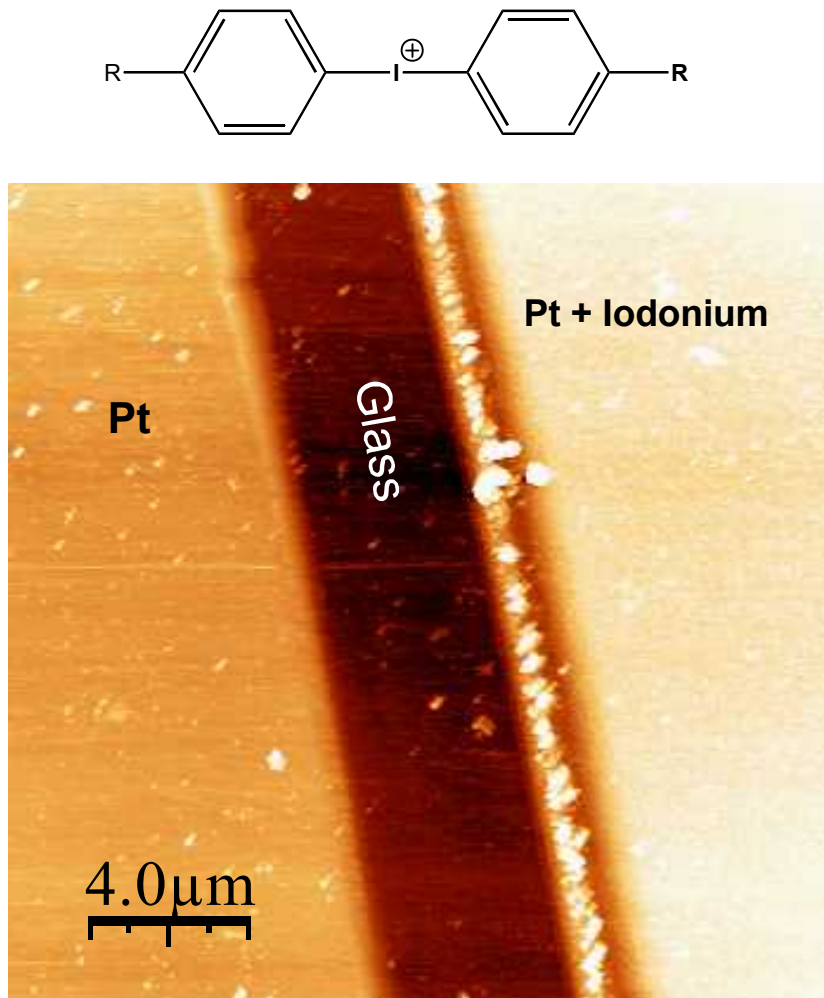
- Phosphonate-selective
- Electron hopping?

Swelling mechanism, nonpolar

- Swelling mechanism
- Vary polarity, polarizability
- Changing partition coefficients adds information to array response, increasing analytical power



Bias-driven Iodonium Reduction Enables Selective Deposition on Electrode Arrays



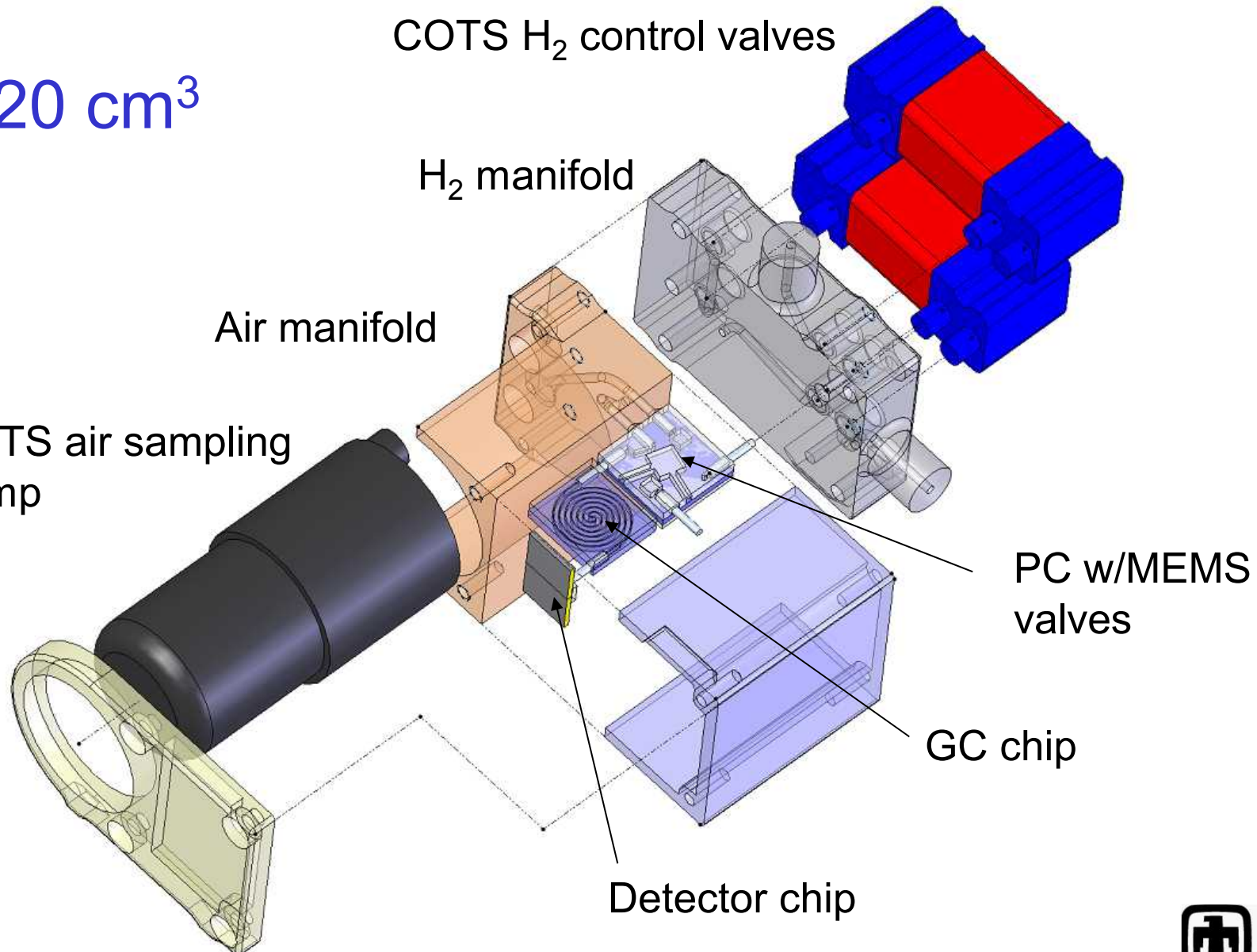
The AFM image shows two isolated Pt electrodes. Iodonium molecules were reduced on the right electrode by application of a voltage.

Shawn M. Dirk, et al., Langmuir 21 (2005) 10899.



Phase 2 MGA System

$< 20 \text{ cm}^3$





Development of Micro Analytical Vapor Sensor Systems: Summary

- For high-consequence analyses, lowering false alarm rate is most important, but...
- Military, domestic counterterrorism, and law enforcement users all want it smaller, faster, lighter, cheaper, lower power, etc. *ad nauseum*
- We can build vapor detection systems based on microanalytical components, that use gas chromatographic separation to achieve low false alarm rates.
- In order to make these faster, smaller, cheaper, and more sensitive, we need:
 - A switch from air carrier to hydrogen for the GC
 - More sensitive, faster detectors
 - New preconcentrators to more efficiently capture target compounds
 - Valves and flow control to integrate the components